LAWRENCE
LIVERMORE
NATIONAL
LABORATORY

UCRL-JRNL-201340

Effects of the Use of Pore Formers on Performance of an Anode supported Solid Oxide Fuel Cell

J. J. Haslam, A-Q. Pham, B. W. Chung, J. F. DiCarlo, R. S. Glass

December 8, 2003

Journal of the American Ceramic Society

Effects of the Use of Pore Formers on Performance of an Anode Supported Solid Oxide Fuel Cell

Jeffery J. Haslam[*], Ai-Quoc Pham, Brandon W. Chung, Joseph F. DiCarlo[1], Robert S. Glass
Lawrence Livermore National Laboratory
Livermore, CA 94550[**]

Abstract

The effects of amount of pore former used to produce porosity in the anode of an anode supported planar solid oxide fuel cell were examined. The pore forming material utilized was rice starch. The reduction rate of the anode material was measured by Thermogravimetric Analysis (TGA) to qualitatively characterize the gas transport within the porous anode materials. Fuel cells with varying amounts of porosity produced by using rice starch as a pore former were tested. The performance of the fuel cell was the greatest with an optimum amount of pore former used to create porosity in the anode. This optimum is believed to be related to a trade off between increasing gas diffusion to the active three-phase boundary region of the anode and the loss of performance due to the replacement of active three-phase boundary regions of the anode with porosity.

---

[1] Presently at Yardney Technical Products, Inc., Pawcatuck, Connecticut 06379-2154

[**]This work was performed under the auspices of the U.S. Department of Energy by the University of California, Lawrence Livermore National Laboratory under Contract W-7405-Eng-48.
This paper includes work presented at the 102nd Annual Meeting of the American Ceramic Society, St. Louis, MO, May 3,2000 (Electrochemical Materials, Processes, and Devices Symposium, Paper No. A3-038-00).

[*] Member of the American Ceramic Society

I. Introduction

It is desirable to improve the performance of solid oxide fuel cells for intermediate and high temperature use to help solid oxide fuel cells meet technical and economic requirements for power production. The performance of solid electrodes for solid oxide fuel cells is related to available surface area for reaction and the ability of reactants to reach the reaction area [1-3]. The rate of the chemical reaction of the fuel and oxygen in the cell can be limited by many effects that show up as polarization of the cell. Polarization causes voltage drops within the electrodes that limit the output voltage of the fuel cell and consequently reduce the area specific output power at a given current density. Sources of polarization can include electrical resistance to current flow, resistance to ionic transport through the electrolyte, kinetics of the reaction at the interfaces, charge-transfer resistance, and polarization due to resistance to diffusion of the gases to the active three-phase boundary reaction regions [2]. Polarization reduces the performance of the fuel cell.

In our previous work, there were indications of gas diffusion limitations on the fuel cell performance for the materials that we use for an anode supported fuel cell. In a thick anode, gas diffusion can be an issue because hydrogen gas (or another fuel gas) is diffusing into the electrode at the same time that the reaction product (water vapor) is diffusing out of the electrode. This is referred to as counter diffusion of hydrogen gas and water vapor. The most common anode material for solid oxide fuel cells starts with a mixture of ceramic particles of nickel oxide and yttria-stabilized cubic zirconia (YSZ), which is partially densified and then reduced to form a nickel/YSZ composite. This article will examine improvements in fuel cell performance of anode supported fuel cells as

measured by increased voltage (or power) at a given current density as a function of added porosity in the anode. The added porosity is a result of pore formers added to the anode during fabrication. We have used several pore formers (in particular other starches) and pore forming approaches (e.g. decomposable nickel salts) but only work with rice starch is reported here.

Many ceramic bodies formed from powders inherently contain pores between particles due to incomplete densification. The porosity is present even without adding pore former to the ceramic particle mixture. The porosity from incomplete densification is a desirable result in fuel cell electrodes. Others previously have examined the effects of using various ceramic particle sizes to control the amount of porosity retained after sintering and to prevent nickel coarsening in the anode during operation [4, 5]. These are approaches for changing the microstructure within the anode; however, they are not as effective at producing large pore pathways within the microstructure particularly when only fine ceramic particles (<1μm) are used to form the anode. Increased polarization in fuel cells has been related to the particle size of the powders used to form the anode due to the difficulty of gas diffusion through small pores left between fine particles [6]. This can particularly be an issue with anode supported designs because the anode is relatively thick. Analytical explanations have been developed which indicate this condition [2] and there is some experimental evidence of polarization associated with water vapor concentration in the anode [7]. Microscopy, porosimetry, and permeability measurements have also been used to study microstructures for thick anode materials [8]. Additional porosity can be produced by adding pore former materials, which decompose to gases during heat treatment processes [9]. These pore formers are often organic

materials. Various materials have been used for this purpose in the anode of solid oxide fuel cells including graphitic carbon [10], short carbon fibers [11], and polymer spheres [12]. Additionally, work has been done to produce tape cast ceramic materials with similar types of pore forming materials [13]. Issues with gas diffusion limiting the current density and consequently the performance of fuel cells have been noted previously for the anode [2]. Although other authors have reported work with various particle size effects for the anode and the use of pore formers in the microstructure, there is not a clear experimental illustration of the influence of quantity of pore former on solid oxide fuel cell performance.

Performance of the anode in an anode supported solid oxide fuel cell depends on more than just the amount of porosity in the anode. In an electrode, a continuous connection of pores is necessary to allow diffusion of reactants to the active reaction area and diffusion of reaction product from the active reaction area. In a nickel/YSZ composite fuel cell anode, there is an effective thickness where reaction occurs next to the electrolyte (the active three-phase boundary reaction area) that can be on the order of 50 to 150 μm [3]. The size of the pores can be important in allowing rapid diffusion of gas (in solid oxide fuel cells) to the active reaction area within the electrodes. Obviously, reducing pore sizes to very fine scales will significantly limit gas diffusion. A large amount of very fine particles can increase the reaction area tremendously, but the diffusion of gas within the fine pores in such an electrode would be relatively slow and limit the overall reaction rate. Conversely, too much porosity or very large pore sizes will reduce the amount of total three-phase boundary area available for reaction since anode particles could otherwise have been present in the locations of the pores. There may also be issues with the isolation of small regions of the anode either

electronically or in terms of the ionic conductivity. Even without complete ionic or electronic isolation, restriction of the ionic or electronic conduction paths will increase polarization in the anode. Considering these possible issues, there must exist some optimum size and amount of porosity for the anode in this fuel cell application.

In this study we focused on effects of added porosity when the porosity is uniformly distributed in the anode. Our approach to evaluate the diffusion of gases within the anode is to examine the progress of the reduction process for the nickel oxide/YSZ anode using thermogravimetric analysis (TGA) in a hydrogen gas atmosphere. In this case the pore formers have already been decomposed and only the nickel oxide is being reduced. Unless the pores are extremely large, this process will be limited by the diffusion of the gases into the bulk material rather than by the reaction rate at the nickel oxide particle surface or the diffusion of gases through the boundary layer of the particle surfaces [14]. A more rapid reduction rate should indicate more effective diffusion of the hydrogen and water vapor within the anode material. Cell performance measurements will be used to compare the amount of polarization of the fuel cell relative to the amount of added porosity.

II. Experimental Procedures

Pore forming materials were selected to provide additional porosity, which improves access to the active three-phase boundary regions of the anode. Criteria for selection included particle size, decomposition with minimal residue at reasonably low temperatures, and compatibility with other materials in the

anode. Several starches and nickel salts were considered. A rice starch was used in the study results presented here. The rice starch has a particle size of about 4 to 5 microns. Particle size was estimated by Scanning Electron Microscopy (SEM) (JEOL 35-CF, Tokyo, Japan) of the dry starch particles coated lightly onto a carbon adhesive tape. A micrograph of the rice starch particles is shown in Figure 1. Examination of the starches milled without powders suggested that no significant reduction in pore former size occurred during milling (the milling is described later). However, the amounts of communition of starch particles milled with ceramic particles and deformation of the starch particles during dry pressing used to fabricate samples were unknown. Thermogravimetric analysis (Model TGA-50, Schimadzu, Inc., Kyoto, Japan) in stagnant air was used to analyze the decomposition of the pore-forming materials. A heating rate of 1°C/minute was used.

Anode samples were prepared by mixing the desired quantities of nickel oxide (J.T. Baker, Phillipsburg, NJ), yttria-stabilized cubic zirconia (YSZ) (8 mole % yttria-zirconia, TZ-8Y, Tosoh, Inc., Tokyo, Japan), and the pore forming material. The ratio of the nickel oxide and YSZ was maintained at 55 weight % nickel oxide and 45 weight % YSZ. These powders were mixed in denatured ethanol and ball-milled for at least 12 hours. The rice starch was not observed to be significantly soluble in alcohol. The weight fractions of starch pore former were based on the weight of starch relative to the amount of total ceramic powder and pore former. Starch density was taken to be 1 g/cc for both starches. The rice starch was used at weight fractions of 10, 20, and 30 weight %. These weight fractions correspond to 41, 61, and 73 volume % pore former

(relative to the total amount of ceramic and pore former). Samples were also produced with the nickel oxide/YSZ mixture without pore formers.

The suspensions were dried after ball milling at less than 80°C to prevent decomposition of the pore forming materials. The resulting dried powder was ground by hand in a mortar and pestle. Quantities of powder to produce a desired thickness of nominally 1 mm were dry pressed in a 22 mm die at 57 MPa. Samples were heated at no more than 1°C/minute to 1000°C to decompose the pore former and then cooled. The samples were then fired at 5°C/minute to 1450°C for 5 minutes and cooled to room temperature at the same rate. For the reduction rate measurements in the TGA, the resulting pellets were cut to dimensions of 2 x 2 x 1 mm. For this part of the study no electrolyte or cathode was present in the samples. (For fuel cell anodes the electrolyte is applied prior to firing at 1450°C.) Samples containing effectively larger and smaller pore formers were analyzed in the reduction rate experiments to provide comparisons to the results for the rice starch. This provided a qualitative validation of pore size effects on the measured reduction rate, but these results are not reported here.

For the reduction rate measurement, the cut samples (after sintering in air at 1450°C) were loaded into the TGA weighing pan, then heated in flowing air to 800°C, and held isothermally during the experiment. The sample size was chosen so that the sample mass would be close to full scale on the weighing balance to improve the resolution of the measurements. Gas flow was controlled by a mass flow controller set at 40 cc/minute. Gas switching between dry air and 4% hydrogen (balance nitrogen) was accomplished with a gas switching device supplied with the TGA. The mechanical gas switching approach

provided for minimal disruption of the stability of the balance due to gas flow changes. Since dry air and the gas mixture of 4% hydrogen in nitrogen have nearly the same coefficients for mass flow meters, the gas flow measurements were easily made with the same meter. The reduction rate was monitored and evaluated by measuring the percent reduction (in the sample mass) with time. The reduction rate was linear soon after the reduction began but departs from linearity after the first few minutes of reduction. The bulk of the reduction occurred in a rapid manner and was typically nearly complete in 20 minutes. An average reduction rate from multiple measurements is reported. Samples were also tested with a smaller sample size. The same trends were observed with the smaller sized samples. A comparison between the rate of reduction with the small samples and the large samples indicated that small differences in the bulk dimensions of the samples should not affect the trend in the measurements with any reasonable significance.

For fuel cell testing, anodes were prepared in a similar manner to the above description. The anodes were fired to intermediate temperatures (1050°C or less) to strengthen them before applying the electrolyte layer. The same yttria-stabilized zirconia (8 mole % yttria) powder mentioned above was used to form the electrolyte. The electrolyte layer was applied by the Colloidal Spray Deposition (CSD) method to a layer thickness that resulted in a 15 μm film of YSZ after firing [15]. The anode and electrolyte were then co-fired to produce an impervious YSZ film on the anode. The cathode material was formed from powders of the same zirconia powder and $La_{0.85}Sr_{0.15}MnO_3$ (LSM) powder (Praxair Specialty Ceramics, Danbury, CT) with an added pore forming material. The LSM powder was ultrasonnicated and sedimented to remove large particles

and agglomerates. The cathode was composed of 55 weight % LSM and 45 weight % YSZ. The cathode was also applied by the CSD method and fired at 1150°C for 1 hour. The nominal thickness was 40 - 50 μm after firing.

The cells were prepared for testing by applying platinum paste (CL11-5100, Heraeus, Inc., West Conshohocken, PA) to cover the cathode and to cover an equal area on the anode surface in a symmetric configuration. A schematic of the cell configuration is shown in Figure 2. A platinum mesh was cut to cover the platinum paste and provide tabs for attaching a current lead and a voltage lead to each electrode surface. The platinum paste was also used to attach a platinum mesh current collector to both electrodes. The samples were heated to 900°C in air to decompose organics in the paste and to form a good electrical bond. Separate wire leads for the current and voltage measurement were attached to the platinum wire mesh with two leads to each current collector. The resulting cell was a flat disk. The disk was placed on an aluminum oxide tube with an interior diameter slightly larger than the current collectors and the disk was sealed to the tube with a multi-layered application of a ceramic seal (Aremco 516 and 571, Aremco Products, Inc., Valley Cottage, NY). The anode side of the cell faced into the interior of the tube and the cathode side of the cell was open to ambient air. The seal was cured by a programmed heating of the entire assembly to 800°C in flowing nitrogen gas on the anode side. The anode was reduced in place initially with 4% hydrogen gas (balance nitrogen). The reduction was completed with pure hydrogen gas, which was also used for cell testing. Cell testing was begun after a stable open circuit voltage was obtained. For testing, the hydrogen gas flow rate was 100 cc/minute (at 25°C) measured by a mass flow controller. Increases in the gas flow rate did not produce significant

changes in the performance of the cell. The cells were conditioned for testing by incrementally changing the load current and waiting for a stable voltage to be obtained. I-V curves were measured starting at a high current and sequentially reducing the current and recording the voltage and current after a stable voltage was obtained. The cells were fractured after testing and the microstructure was examined by Scanning Electron Microscopy (SEM).

III. Results

The relative densities of the fired samples are shown in Table 1. The table also shows the shrinkage of the materials. Although the shrinkage was greater with more pore former present, the amount of porosity retained in the samples was still greater when more pore former was used. If the composite anode does not shrink during the reduction, an additional amount of porosity will be created based on the volume of the nickel oxide originally present. In this study, the amount of nickel oxide was fixed at 55 weight %, which would produce 21 volume % additional porosity if no additional shrinkage occurs during the reduction.

Thermogravimetric analysis of the decomposition of the rice starch pore former was performed at 1°C/minute. This is shown in Figure 3. The rice starch typically loses water initially and decomposes between 200 and 400°C.

A typical measurement of the reduction rate of the nickel oxide in anode samples is shown in Figure 4. These measurements are performed after the pore formers have been decomposed and after the anode samples were sintered to 1450°C. The initial linear slope after the beginning of reduction was reported as

the reduction rate in percent mass of the sample per minute. Figure 4 shows the reduction of an anode sample that contained pores formed by 20 weight % of rice starch as a pore former. The region for calculation of the reduction rate is the initial reduction portion of the curve. A tangent line is drawn in the figure showing the slope associated with the reduction rate measured.

The average reduction rate (of nickel oxide) in anode samples increases with the amount of rice starch pore former used to form pores as shown in Figure 5. Relative to the plain anode sample, the reduction rate increases moderately with 10 weight % addition and then more dramatically with larger weight fractions of the starch. Examples of the microstructures are shown in Figure 6. The micrographs show that the rice starch produced pores that were approximately 2+ μm in the final microstructure.

Cell performance at 800°C was obtained for fuel cells with the plain anode and with 10, 20, and 30 weight % of rice starch used as a pore former in the anode. Current density – Voltage (I-V) curves and power density curves are shown in Figure 7. The normalizing area was 1.5 cm^2. The trend in performance shows that increasing the amount of pore former reduced the polarization in the fuel cell when up to 20 weight % of the rice starch was used as a pore former. The cell that had 30 weight % rice starch as a pore former in the anode showed decreased performance relative to the 20 weight % rice starch cell. Impedance measurements showed a high-frequency intercept resistance of approximately 100 milliohms for each of the samples at 800°C. A micrograph of a fuel cell in cross-section (fracture surface) is shown in Figure 8. Although not reported here, the fuel cells were also tested at temperatures below 800°C and a similar trend

was observed in the relative performance of the cells with the differing amounts of pore former used to form porosity in the anode. The maximum power densities decreased at lower temperatures as expected. The performance of the fuel cell with 30 weight % rice starch used as a pore former was always less than the one that used 20 weight % of the rice starch. The performance of the cell with 20 weight % rice starch used as a pore former was greater than the others cells at all the test temperatures.

IV. Discussion

The reduction rate measurements show a clear trend of increasing reduction rate with increasing amounts of added porosity (due to the rice starch pore former) in the anode. Larger amounts of added porosity should reasonably allow for more hydrogen gas diffusion into the microstructure and for diffusion of the water vapor reaction product from the anode. In the fuel cell, greater diffusion provides for greater access to and from the active three-phase boundary regions where the reactions occur and therefore should reduce polarization due to gas diffusion resistance. Figure 5 shows that this trend is very pronounced with increasing amounts of the rice starch pore former. The 10 weight % rice starch sample had only a marginal increase in reduction rate measurement. This amount of added pore former increased gas diffusion in the anode although the increase was not enough to produce a large change in the reduction rate measurement. Percolation effects could play a role here and an interpretation would require consideration of the densification of the anode prior to reduction. However, even 10 weight % of pore former did have a significant

effect on cell performance as shown in Figure 7. Added porosity does not directly increase the internal surface area for chemical reaction. Therefore, the increased fuel cell performance for the 10 weight % rice starch anode fuel cell indicates that gas diffusion was significantly limiting the fuel cell performance in the fuel cell with the plain anode (no added porosity in the anode). Increasing amounts of porosity resulting from the added pore former can be seen on the fracture surfaces of the rice starch pore former samples in Figures 6 (b) - (d). The increasing amounts of porosity, particularly with 20 and 30 weight % rice starch used in the anode, did clearly increase the reduction rate measurements as shown in Figure 5. These results indicate increased gas diffusion rates in anodes with additional porosity created by pore formers.

For the purposes of the following discussion, different amounts of polarization will be attributed to the differences in the I-V behavior between cells at a current density within the ohmic region of the I-V curve (linear I –V region). Reduction in polarization can be observed as higher voltages at current densities above 0.5 A/cm^2 on the I-V plots in Figure 7 for fuel cells with added porosity in the anode. The polarization when using the anode that had additional porosity created by 10 weight % of rice starch was significantly less than with the plain anode. The lower polarization leads to a higher maximum power density obtained when the pore former was added. This occurred even though the reduction rate measurements and the total porosity in the 10 weight % anode were not much larger than in the plain anode. However, even the relatively small additional volume of large pores added to the microstructure by the pore former improved gas diffusion within the anode. This apparently produced significantly lowered polarization within the anode, and consequently increased

cell performance, even without a substantial increase in total porosity. This reduction of polarization due to the added porosity from pore formers could increase the effective thickness of the active three-phase boundary region in the anode and thereby improve the cell performance. Both effects would produce increased current density at a given cell potential (and similarly, an increased cell potential at a given current density). The existence of a few larger pores from the pore former can be observed in Figure 6 (b) compared to the plain anode in Figure 6 (a).

The fuel cell performance was even greater in the cell with additional porosity created in the anode by 20 weight % of rice starch, which can be observed to have even more added porosity in Figure 6 (c). Again, the magnitude of the improvement in the fuel cells (due to reduced polarization) with increased amounts of porosity from pore formers strongly suggests that the gas diffusion within the anode is significantly limiting the performance of the fuel cells in this work. In Figure 7 it can be seen that the addition of porosity produced by up to 20 weight % of rice starch increased the current density at which the performance of cells (power and cell voltage) begins to precipitously drop off. In the fuel cells with added anode porosity from the pore former this occurs at 2 – 3 A/cm^2 compared to 1.5 A/cm^2 in the plain anode fuel cell. We attribute this precipitous drop in performance to limitations on the transport of gases through the anode.

In the fuel cell with porosity in the anode created by 30 weight % of rice starch, the amount of polarization was greater than when 20 weight % of the pore former was used and consequently the power density obtained was lower. Based on the reduction rate measurements, the 30 weight % rice starch anode

might have been expected to have lower polarization due to greater rates of gas diffusion to the three-phase boundary area. The decrease in cell performance (relative to the cell with porosity created from 20 weight % rice starch) is attributed to the excessive replacement of active three-phase boundary area with porosity. The added porosity decreases the current density because the lost reaction area does not directly contribute to the cell performance. In the case of the anode with porosity created by a 30 weight % addition of rice starch, the reduction in polarization due to an improvement in gas diffusion is overwhelmed by the polarization associated with a loss of active three-phase boundary area. This effect can be expected by considering that the large pores shown in Figure 6 (d) would exist in the effective thickness of the three-phase boundary reaction area adjacent to the electrolyte and consequently remove some of the available surface area for chemical reaction.

An additional effect of added porosity may be that small regions of the active three-phase boundary area can loose (or have diminished) electrical connectivity to the remainder of the anode due to the presence of a pore where there otherwise would have been nickel metal particles to provide electrical connection. Pores may also disrupt the oxygen ion diffusion pathways from the YSZ in the anode to the YSZ electrolyte and consequently produce "ionic" isolation or diminished ionic conductivity in regions of the anode [16]. Features in the 30 weight % rice starch pore former anode microstructure in Figure 6 (d) would support this conclusion. The optimum amount of porosity for this anode composition and microstructure should exist somewhere between the amount of porosity obtained when 10 and 30 weight % of the rice starch is used as a pore former.

V. Summary

The reduction rate measurements combined with fuel cell I-V performance measurements suggest that larger amounts of pore former used during anode fabrication increases the gas diffusion within the fuel cell anodes used in this work. The added porosity is particularly effective in reducing polarization in the anode supported fuel cell because of the importance of gas diffusion in the relatively thick anode. The reduction rate measurements were consistent with the porosity observed in the microstructures by scanning electron microscopy and the measured relative densities of the anodes before reduction. Increasing the amount of porosity in the anode microstructure improved performance in the fuel cell at 800°C. However, we believe removal of active three-phase boundary region due to excessive replacement of the anode material with pores decreases the cell performance. In this study, this occurred in the case of the anode with 30 weight % of rice starch used as a pore former even though the reduction rate measurements would suggest greater gas diffusion within the anode. Consequently, there exists an optimum amount of added porosity for fuel cell performance.

VI. References

[1] N. Q. Minh, "Ceramic Fuel Cells," J. Am. Ceram. Soc., **76** [3] 563 - 588 (1992).

[2] J. Kim, A. V.Virkar, K. Fung, K. Mehta, and S. C. Singhal, "Polarization Effects in Intermediate Temperature, Anode-Supported Solid Oxide Fuel Cells," J. Electrochemical Soc. **146** [1] 69-78 (1999).

[3] A. Abudula, M. Ihara, H. Komiyama, and K. Yamada, "Oxidation mechanism and effective anode thickness of SOFC for dry methane fuel," Solid State Ionics **86-88** 1203-1209 (1996).

[4] S. Murakami, Y. Akiyama, N. Ishida, T. Yasuo, T. Saito, and N. Furukawa, "Development of a Solid Oxide Fuel Cell with Composite Anodes"; pp. 105-112 in Proceedings of the Second International Symposium on Solid Oxide Fuel Cells, July 2-5, 1989, (SOFC II).

[5] H. Itoh, T. Yamamoto, M. Mori, and T. Abe, "Sintering Behavior and Performance of Anode Materials for SOFC"; pp. 639-648 in Proceedings of the Fourth International Symposium on Solid Oxide Fuel Cells (SOFC-IV), (Yokohama, Japan, 18-23 June 1995). Edited by: Dokiya, M.; Yamamoto, O.; Tagawa, H.; Singhal, S.C. Electrochemical Society, Pennington, NJ, 1995.

[6] M. Watanabe, H. Uchida, M. Shibata, N. Mochizuki, and K. Amikura, "High Performance Catalyzed-Reaction Layer for Medium Temperature Operating Solid Oxide Fuel Cells," J. Electrochem. Soc. **141** [2] 342-346 (1994).

[7] M. Nagata and H. Iwahara, "Measurement of Water Vapor Pressure in the Vicinity of Anode of SOFC during Discharge"; pp. 829-838 in Science and Technology of Zirconia V, (Melbourne, Australia, 16-21 August 1992). Edited by Badwal, S.P.S., Bannister, M.J., and Hannink, R.H.J. Technomic Publishing Company, Lancaster, PA, 1993.

[8] D. Simwonis, A. Naoumidis, F. J. Dias, J. Linke, and A. Moropoulou, "Material characterization in suport of the development of an anode substrate for solid oxide fuel cells," J. Mater. Res., **12** [6] 1508-1518 (1997).

[9] K. Ishizaki, S. Komarneni, and M. Nanko, Porous Materials Process Technology and Applications. Dordrecht, The Netherlands: Kluwer Academic Publishers, 1998, p. 34.

[10] P. K. Srivastava, T. Quach, Y. Y. Duan, R. Donelson, S. P. Jiang, F. T. Ciacchi, S. P. S. Badwal, "Electrode supported solid oxide fuel cells: Electrolyte films prepared by DC magnetron sputtering," Solid State Ionics **99** 311-319 (1997).

[11] W. Huebener, H. U. Anderson, Harlan U., D. M. Reed, and S. R. Sehlin, X. Deng, "Microstructure <-> Property Relationships of Ni:ZrO_2 Anodes," Solid Oxide Fuel Cells 1995, 696 - 705 (1995).

[12] Moon, J.W. Lee, H.W., Kang, H.G., Kim, J.D., Kim, G.D., and Lee, H.L., "Fabrication of Electrode/Electrolyte Layer with Novel Microstructure using Artificial Pore Former"; pp. 282-91 in Proceedings of the Fourth International Symposium on Solid Oxide Fuel Cells (SOFC-IV), (Yokohama, Japan, 18-23 June 1995). Edited by: Dokiya, M.; Yamamoto, O.; Tagawa, H.; Singhal, S.C. Electrochemical Society, Pennington, NJ, 1995.

[13] S. F. Corbin and P. S. Apté, "Engineered Porosity via Tape Casting, Lamination and the Percolation of Pyrolyzable Particles," J. Am. Ceram. Soc. **82** [7] 1693-701 (1999).

[14] J. W. Evans, S. Song, and C. E. Leon-Sucre, "The Kinetics of Nickel Oxide Reduction by Hydrogen; Measurements in a Fluidized Bed and in a Gravimetric Apparatus," Metall. Trans. B 7B 55-65 (March 1976).

[15] A.-Q. Pham, T. H. Lee, and R. S. Glass, "Colloidal Spray Deposition Technique for the Processing of Thin Film Solid Oxide Fuel Cells," in Solid Oxide Fuel Cells VI, Electrochemical Society Proceedings **99** 172-178 (1999).

[16] C. S. Tedman, H. S. Spacil, and S. P. Mitoff, "Cathode Materials and Performance in High-Temperature Zirconia Electrolyte Fuel Cells," J. Electrochem. Soc., **116** [9] 1170 - 1175 (1969).

Table 1. Properties of anodes as a result of the use of various pore formers

Anode Material	Relative Density after Firing in Air (%)	Linear Shrinkage (%)
Plain	90.9	19.0
10 wt % Rice Starch	88.5	24.3
20 wt % Rice Starch	71.2	24.6
30 wt % Rice Starch	63.4	28.5

VII. List of Figures

Figure 7. Performance of single cells tested with different anodes that had rice starch as a pore former: plain (no pore former), 10 weight %, 20 weight %, and 30 weight %. Open symbols are the power density and the filled symbols are the corresponding I-V curve for the powder density curve with the same symbol shape.

Figure 8. Fracture surface of fuel cell with 20 weight % rice starch in the anode: anode (bottom), 15 μm zirconia (8 mole % yttria) electrolyte (middle), and cathode (top).

Figures.

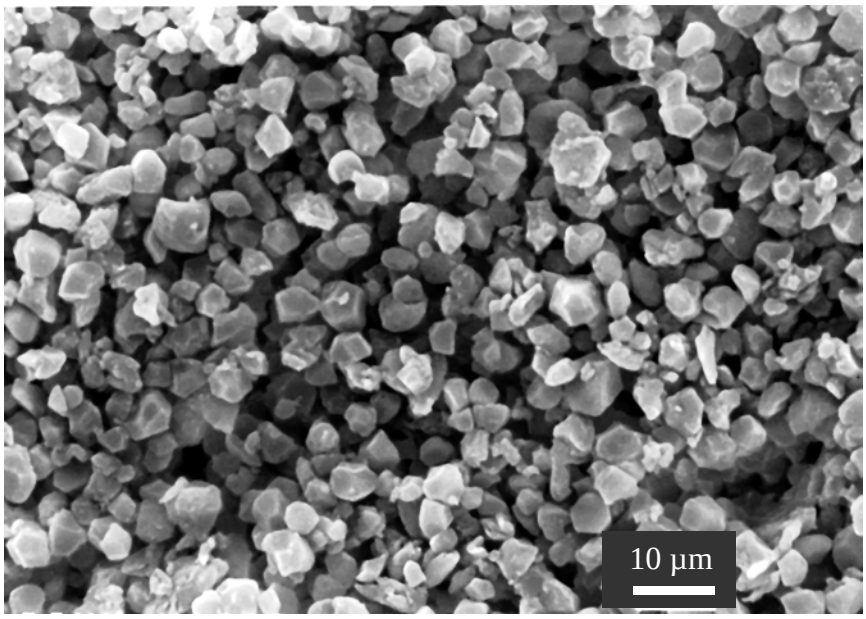

Figure 1. Micrograph of rice starch particles used as pore formers.

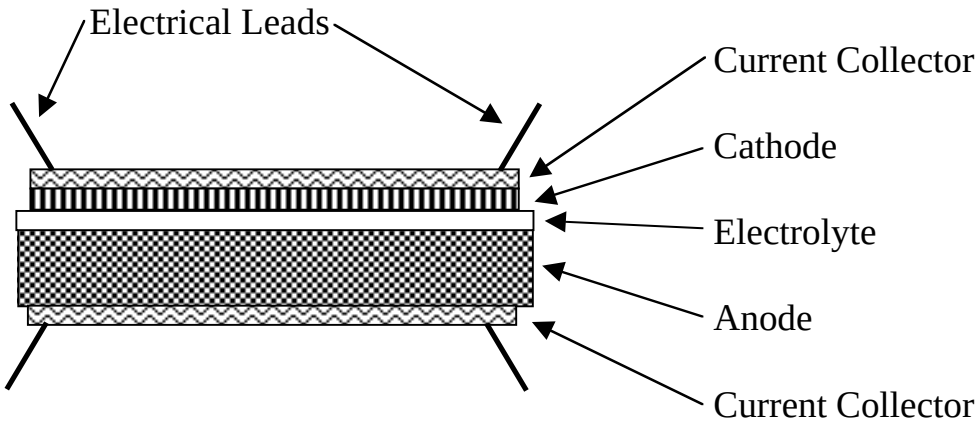

Figure 2. Schematic of fuel cell configuration

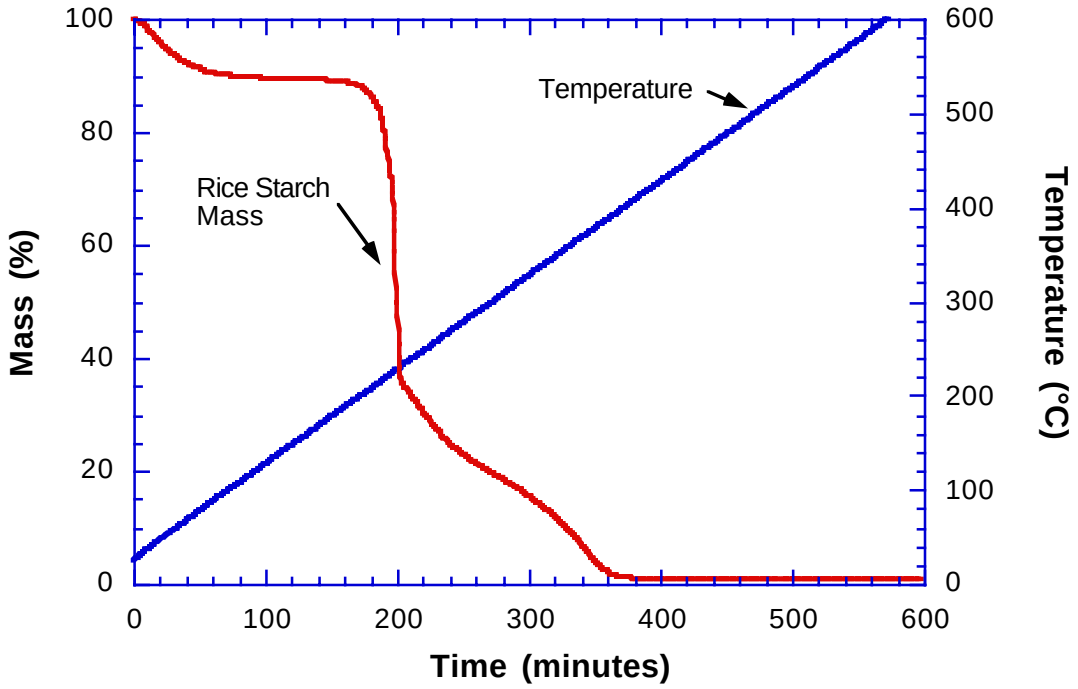

Figure 3. Decomposition of rice starch measured by thermal gravimetric analysis.

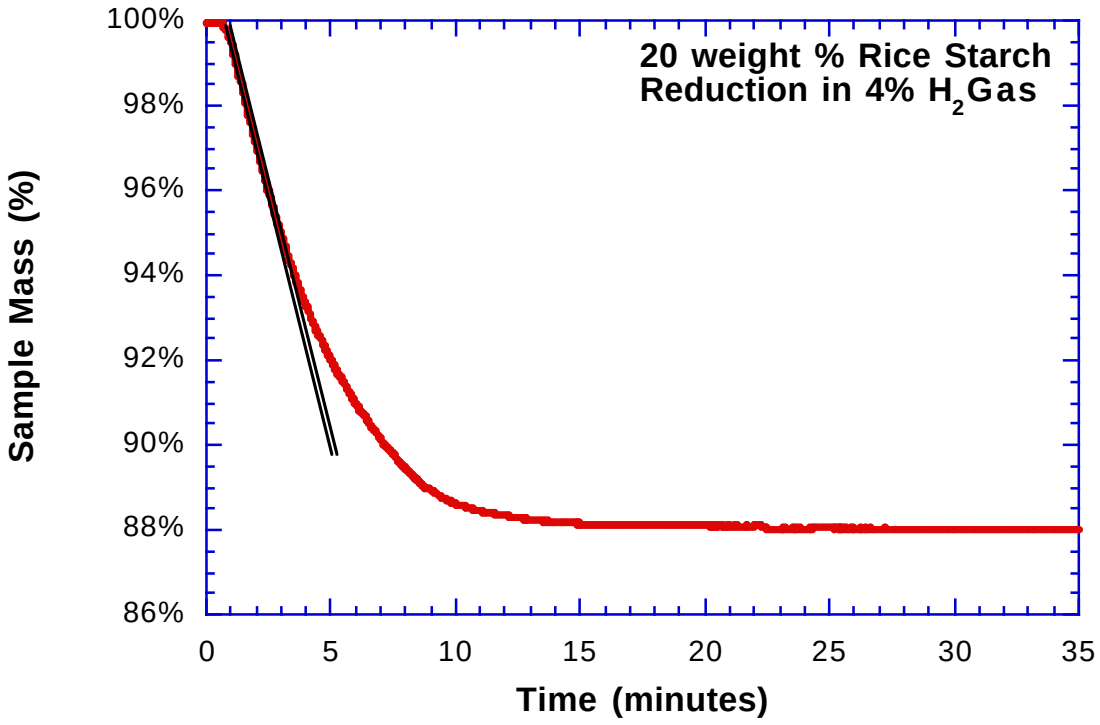

Figure 4. Reduction rate measurement is shown for anode sample with 20 weight % of rice starch with line indicating reduction rate measurement.

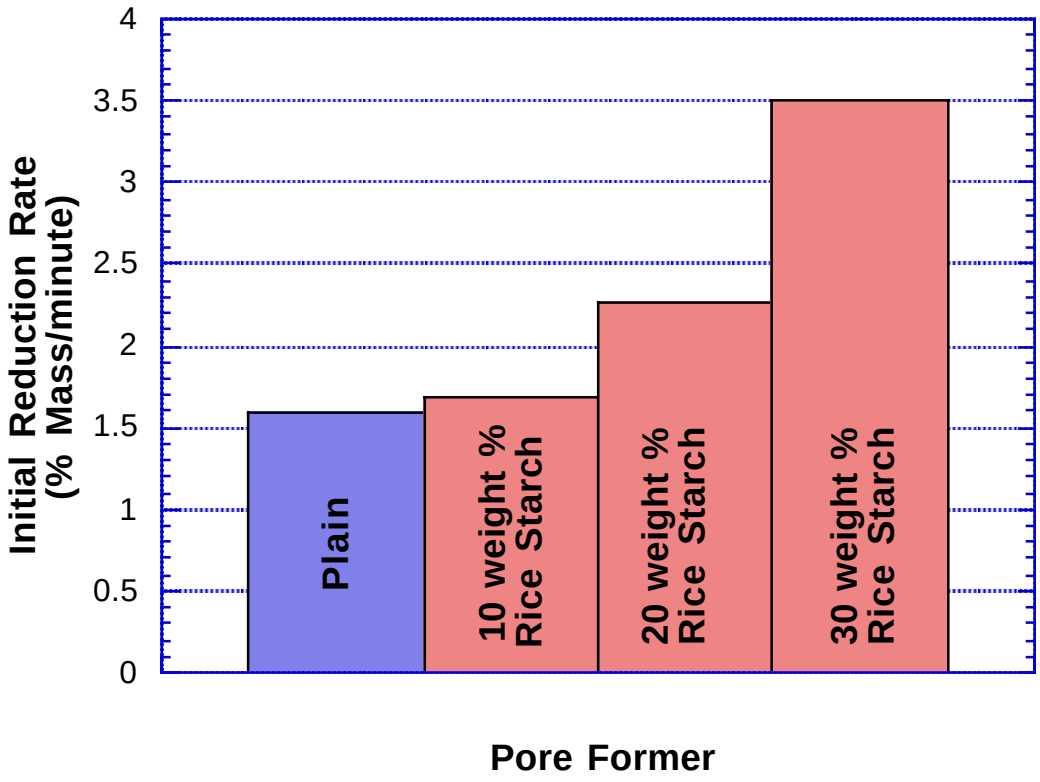

Figure 5. Comparison of the reduction rates for anode samples with various amounts of pore former (no pore former in plain sample).

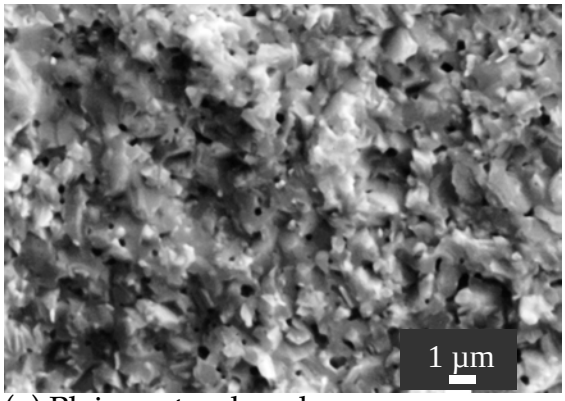

(a) Plain, not reduced

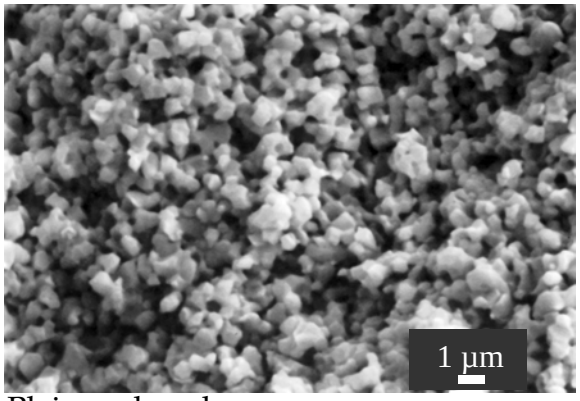

Plain, reduced

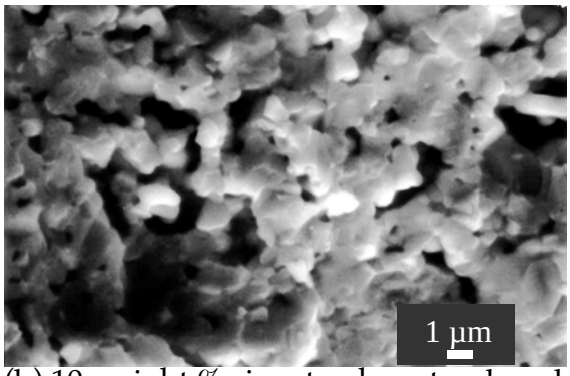

(b) 10 weight % rice starch, not reduced

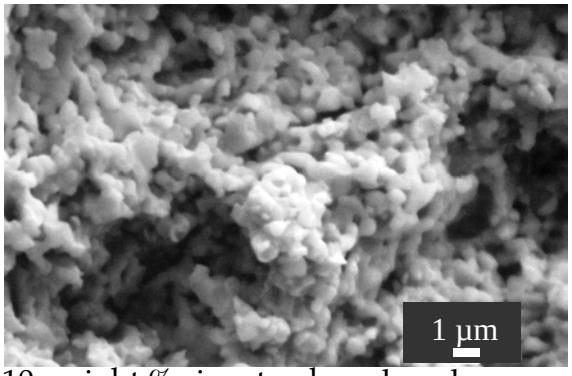

10 weight % rice starch, reduced

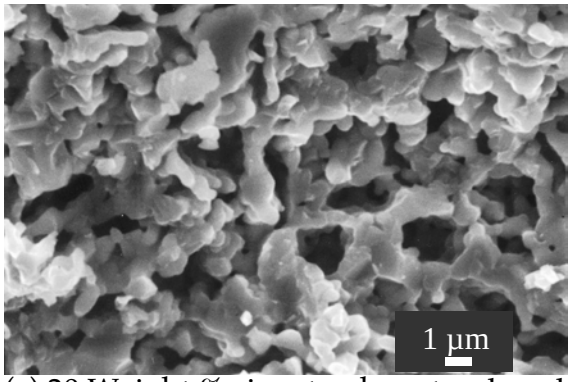

(c) 20 Weight % rice starch, not reduced

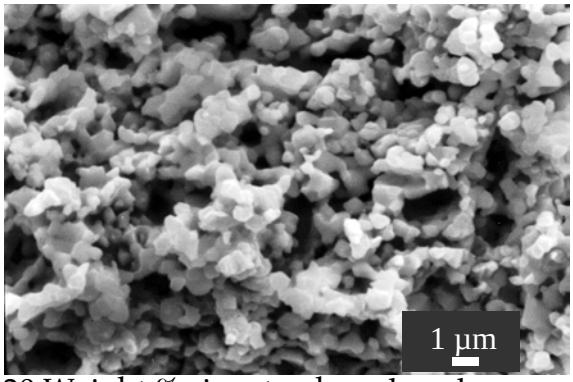

20 Weight % rice starch, reduced

Figure 6. (a) Plain anode microstructure without any pore former, (b) 10 weight % rice starch pore former, (c) 20 weight % rice starch pore former

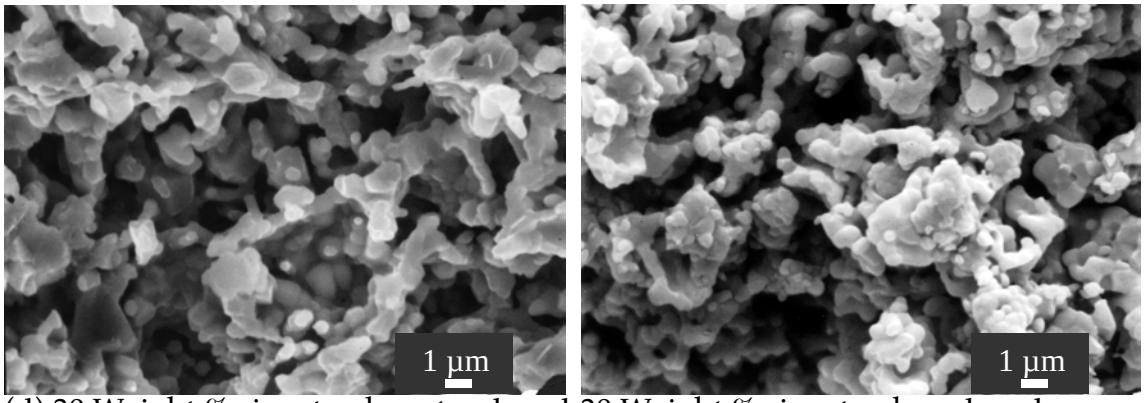

(d) 30 Weight % rice starch, not reduced 30 Weight % rice starch, reduced

Figure 6 (continued). (d) 30 weight % rice starch pore former

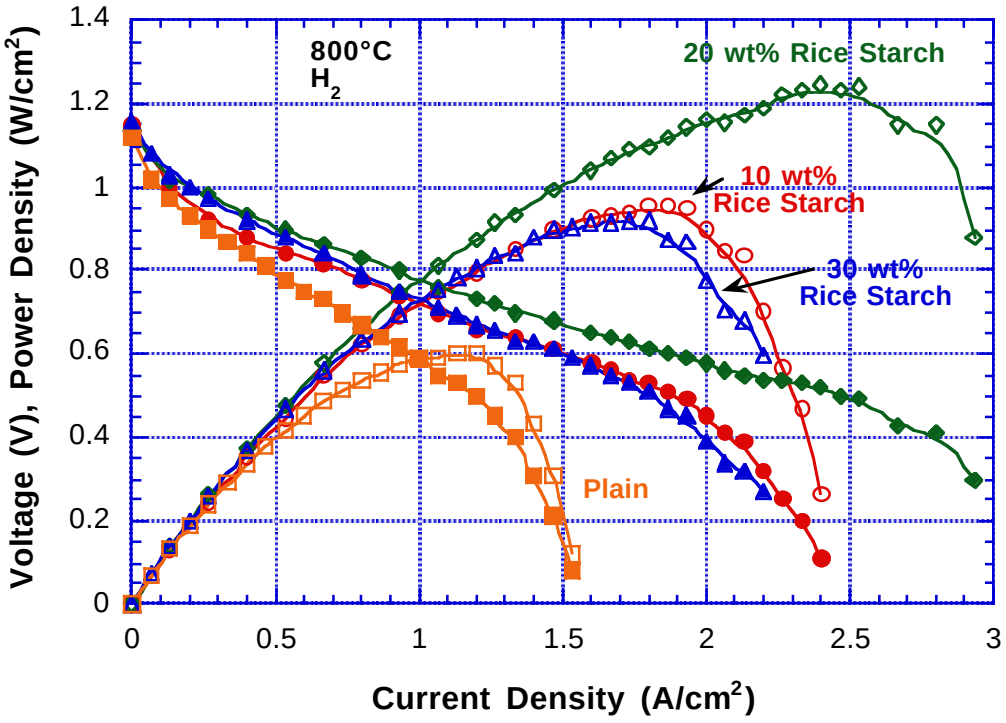

Figure 7. Performance of single cells tested with different anodes that had rice starch as a pore former: plain (no pore former), 10 weight %, 20 weight %, and 30 weight %. Open symbols are the power density and the filled symbols are the corresponding I-V curve for the powder density curve with the same symbol shape.

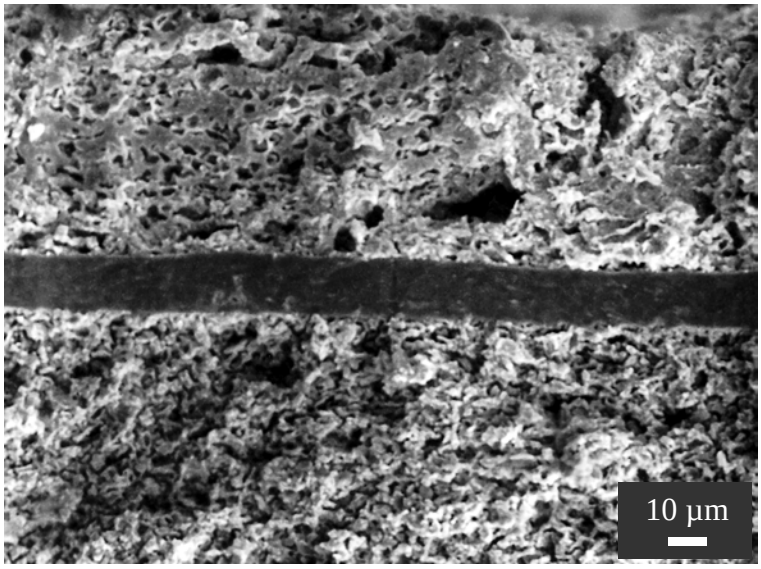

Figure 8. Fracture surface of fuel cell with 20 weight % rice starch in the anode: anode (bottom), 15 μm zirconia (8 mole % yttria) electrolyte (middle), and cathode (top).